

Fig. S1. A. Log transformed graph comparing middle diameter, D_{middle} to body mass for *L. terrestris* and *E. fetida*. B. Log transformed graph comparing posterior diameter, $D_{\text{posterior}}$ to body mass for *L. terrestris* and *E. fetida*. The regressions shown in 3A and 3B were fit to empirical data using OLS regression (solid line for *L. terrestris*, dashed line for *E. fetida*), and the regression equations for both species are shown. * Indicates a significant difference between species with the Bonferroni correction. N=25 per species.

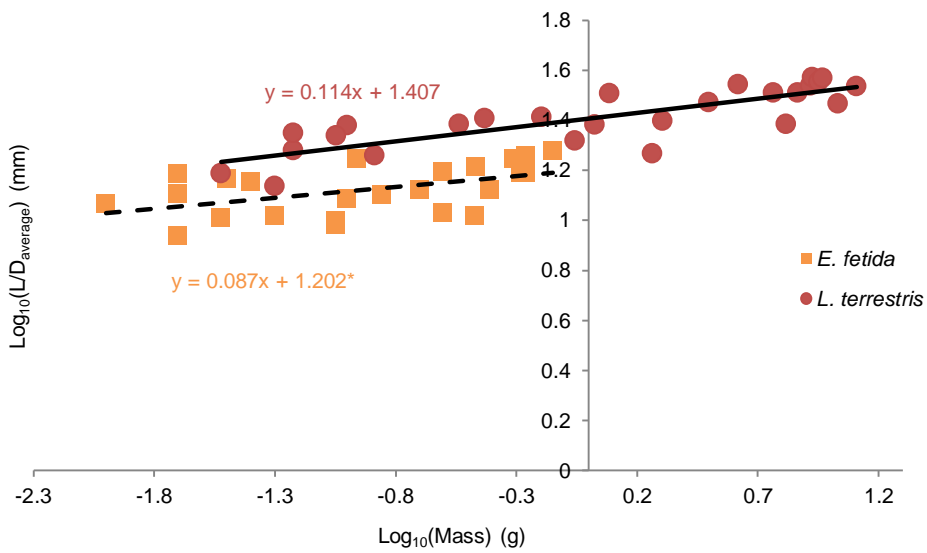


Fig. S2. Log transformed graph comparing the (length/ average diameter) ratio to body mass between *L. terrestris* and *E. fetida*. The regressions were fit to empirical data using OLS regression (solid line for *L. terrestris*, dashed line for *E. fetida*), and the regression equations for both species are shown. * Indicates a significant difference between species with the Bonferroni correction. N=25 per species.

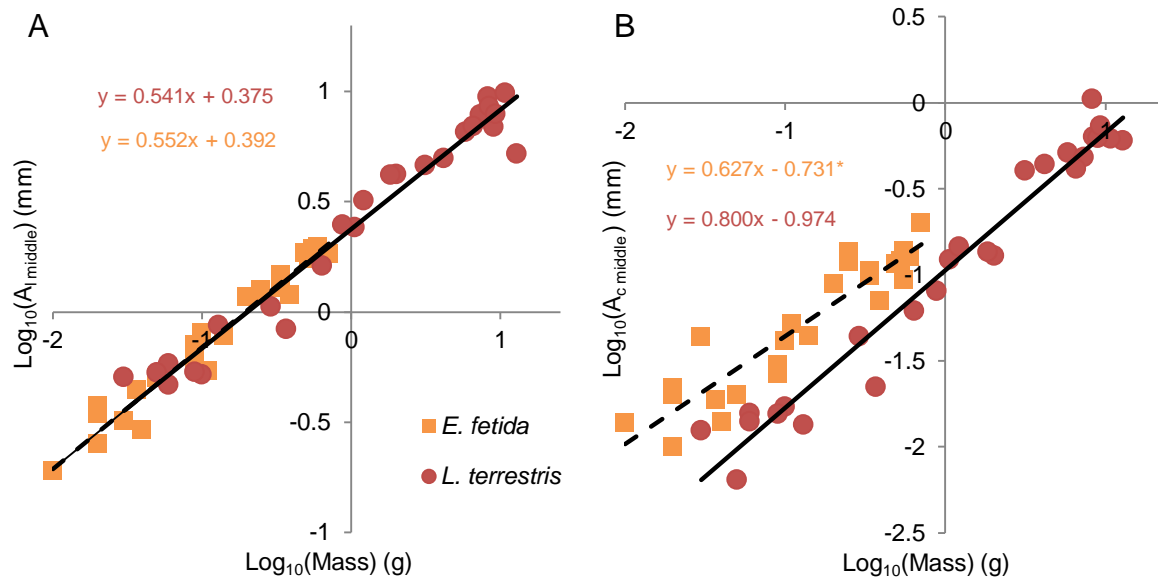


Fig. S3. Ontogenetic scaling of muscle cross-sectional areas in the middle segments. $A_{1 \text{ middle}}$ and $A_{c \text{ middle}}$ refer to longitudinal muscle and circumferential muscle cross sectional areas in the middle segments, respectively. A. Log transformed graph comparing $A_{1 \text{ middle}}$ to body mass for *L. terrestris* and *E. fetida*. B. Log transformed graph comparing $A_{c \text{ middle}}$ to body mass for *L. terrestris* and *E. fetida*. The regressions shown in 1A and 1B were fit to empirical data using OLS regression (solid line for *L. terrestris*, dashed line for *E. fetida*), and the regression equations for both species are shown. * Indicates a significant difference between species with the bonferroni correction. N=25 per species.

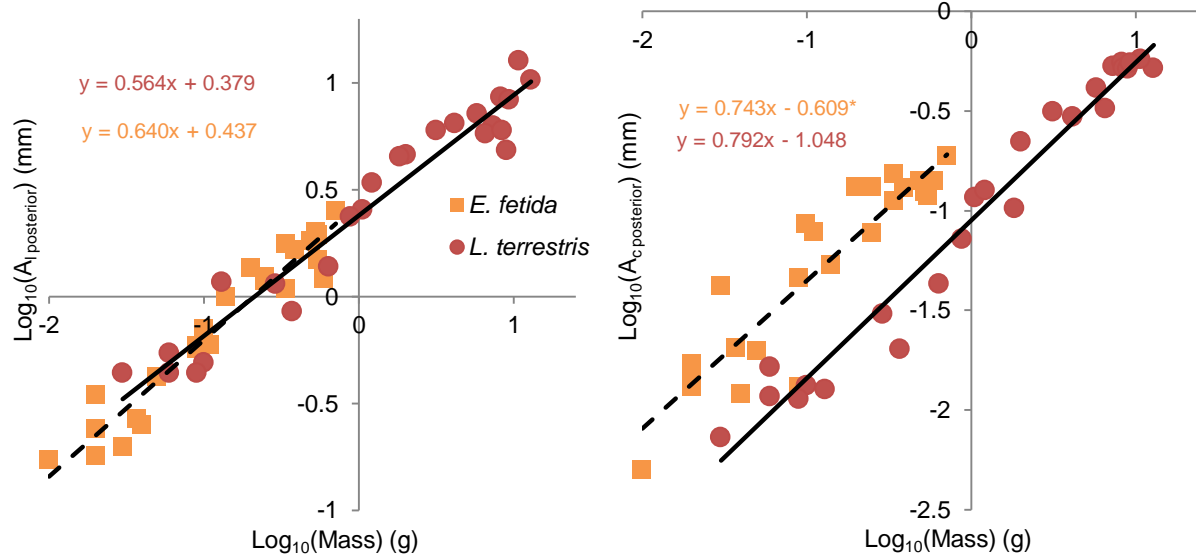


Fig. S4. Ontogenetic scaling of muscle cross-sectional areas in posterior segments. $A_{l \text{ posterior}}$ and $A_{c \text{ posterior}}$ refer to longitudinal muscle and circumferential muscle cross sectional areas in the posterior segments, respectively. A. Log transformed graph comparing $A_{l \text{ posterior}}$ to body mass for *L. terrestris* and *E. fetida*. B. Log transformed graph comparing $A_{c \text{ posterior}}$ to body mass for *L. terrestris* and *E. fetida* in the anterior segments. The regressions shown in 1A and 1B were fit to empirical data using OLS regression (solid line for *L. terrestris*, dashed line for *E. fetida*), and the regression equations for both species are shown. * Indicates a significant difference between species with the Bonferroni correction. N=25 per species.

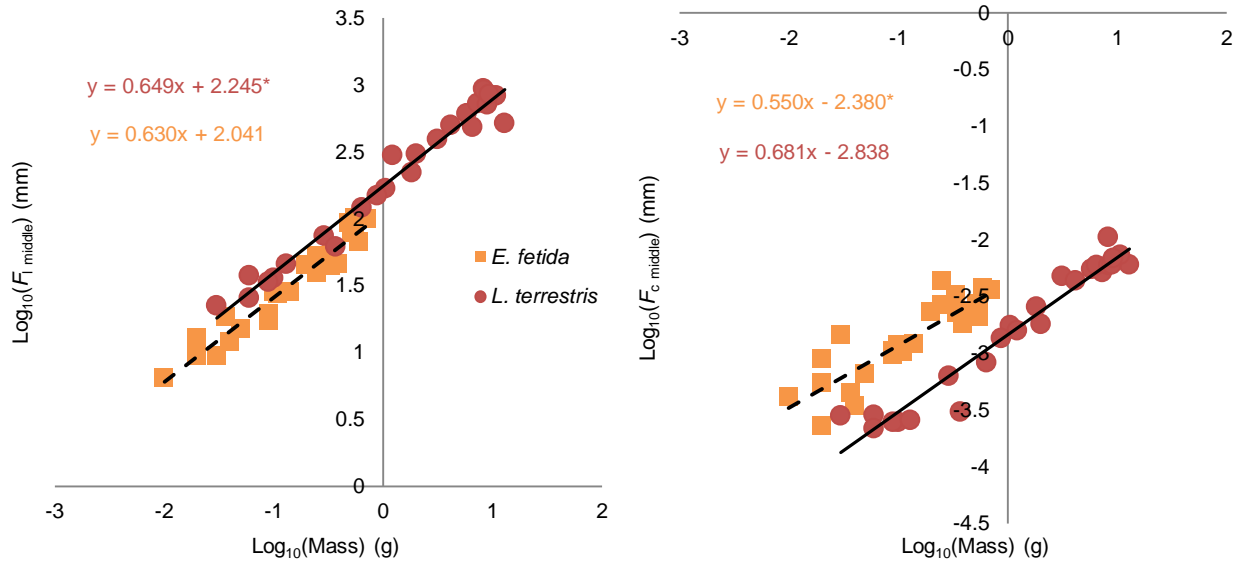


Fig. S5. Comparison of calculated force production with body mass in the middle segments. Force production was estimated for each worm using its mechanical advantage and muscle cross-sectional area. (A) Force production during longitudinal muscle contraction ($F_{1\text{ middle}}$) and (B) force production during circumferential muscle contraction ($F_{c\text{ middle}}$) as a function of earthworm body mass. * Indicates a significant difference between species with the Bonferroni correction. N=25 per species.

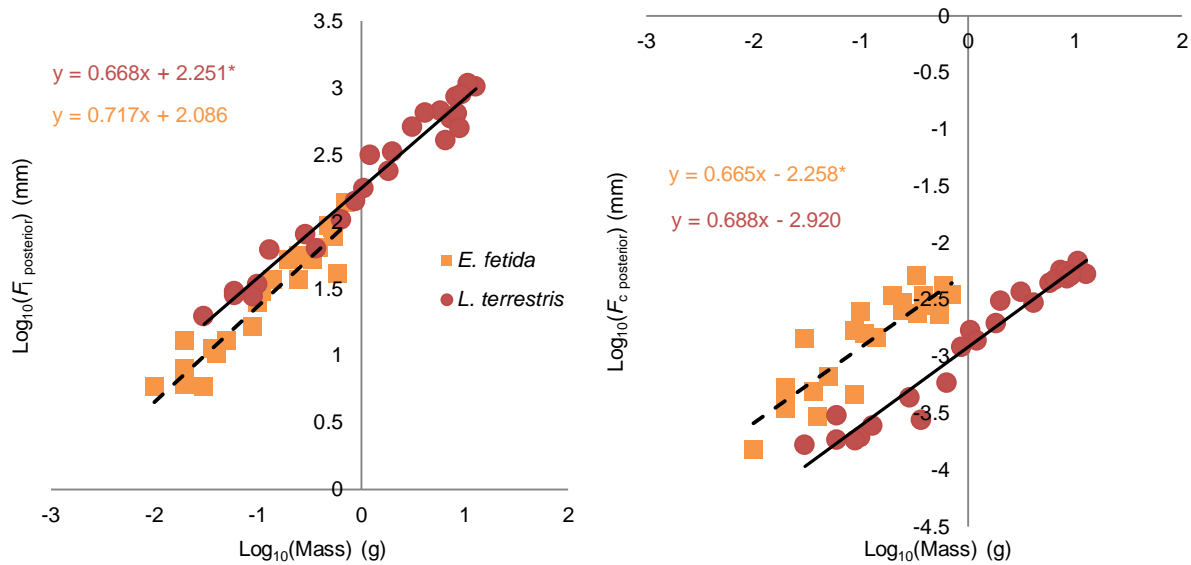


Fig. S6. Comparison of calculated force production with body mass in the posterior segments. Force production was estimated for each worm using its mechanical advantage and muscle cross-sectional area. (A) Force production during longitudinal muscle contraction ($F_{l\text{ posterior}}$) and (B) force production during circumferential muscle contraction ($F_{c\text{ posterior}}$) as a function of earthworm body mass. * Indicates a significant difference between species with the Bonferroni correction. N=25 per species.

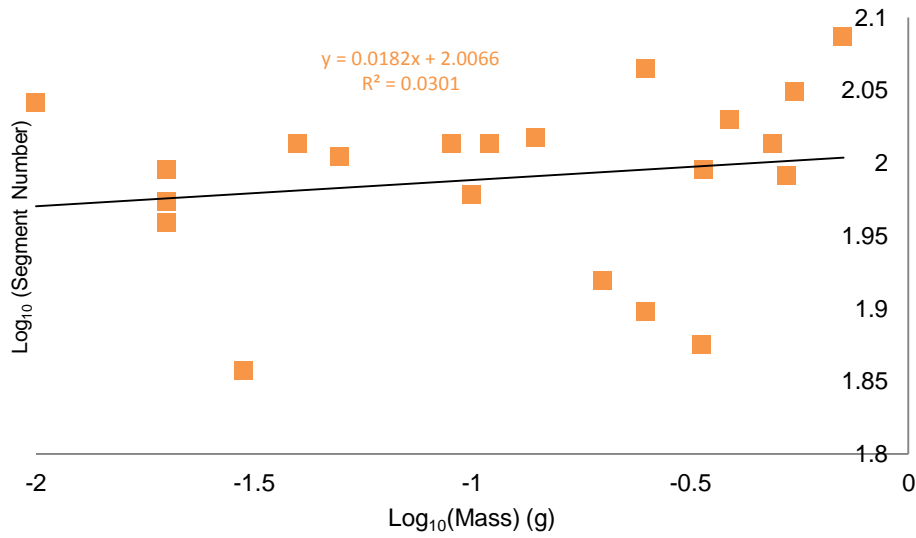


Fig. S7. Log transformed graph comparing segment number to body mass in *E. fetida*. The regression was fit to empirical data using OLS regression and compared with a null slope of zero. * Indicates a significant difference in slope from zero. N=21.